AMERICAN SOCIETY FOR MICROBIOLOGY | Journal of Bacteriology®

MINIREVIEW

Evolution of the Stator Elements of Rotary Prokaryote Motors

Yu-Wen Lai,[a] Pietro Ridone,[a] Gonzalo Peralta,[a] Mark M. Tanaka,[a] Matthew A. B. Baker[a]

[a]School of Biotechnology and Biomolecular Sciences, UNSW, Kensington, Australia

ABSTRACT The bacterial flagellar motor is driven by an ion flux that is converted to torque by motor-attendant complexes known as stators. The dynamics of stator assembly around the motor in response to external stimuli have been the subject of much recent research, but less is known about the evolutionary origins of stator complexes and how they select for specific ions. Here, we review the latest structural and biochemical data for the stator complexes and compare these with other ion transporters and microbial motors to examine possible evolutionary origins of the stator complex.

KEYWORDS flagellar motility, chemotaxis, emergent complexity, evolution, ion channels, secretion systems, stators, *Archaea*, flagellar gene regulation, flagellar structure

The machinery behind microbial swimming is an astounding example of natural nanotechnology. The *Escherichia coli* flagellar motor is currently the best-understood system for bacterial locomotion. It is the product of ~50 genes distributed over 10 operons—of which half encode motor-incorporated proteins and half encode proteins with auxiliary and regulatory functions (1). The bacterial flagellar motor (BFM) structure and amino acid sequence of constituent proteins are conserved across a diverse range of taxa that colonize diverse terrestrial, marine, and commensal environments (2–4). The presence of the BFM across such a wide range of bacterial taxa and environments suggests both an early origin and a significant fitness advantage that is maintained even in nonaqueous environments (5).

The stator complexes are motor-associated protein complexes which convert potential energy, in the form of an ion motive force, to torque. The majority of BFMs are powered by protons or sodium ions flowing across the plasma membrane, but the ion used to power rotation varies across different species, and the mechanism whereby the BFM selectively filters ions is yet to be fully determined.

When investigating the origins of microbial motility, it behooves us also to consider the rotary motors that drive swimming in some species of archaea. Recently, much progress has been made in structural and biophysical characterization of archaeal flagellar motors (AFMs) in *Thermococcus kodakarensis*, *Pyrococcus furiosus*, *Sulfolobus acidocaldarius*, *Methanocaldococcus jannaschii*, *Halobacterium salinarum*, and *Haloferax volcanii* (6). These motors share homology to type IV pili and the homologous type II secretion system (T2SS), rather than the type III secretion system (T3SS), which shares homology with the BFM. The AFM differs from the BFM in the structure of the rotor and filament and, notably, in being powered by ATP hydrolysis rather than ion transit. However, both motors are coupled to conserved chemotaxis machinery which relies on the phosphorylation of CheY (7). The surprising outcome that the chemotaxis machinery is highly conserved, while large structural and functional differences exist between the motors, presents rotary motility as an excellent case study in convergent evolution.

Here, we review the origin and diversity of the BFM, focusing specifically on the stator complexes. We summarize what is known about the genetic and structural

Citation Lai Y-W, Ridone P, Peralta G, Tanaka MM, Baker MAB. 2020. Evolution of the stator elements of rotary prokaryote motors. J Bacteriol 202:e00557-19. https://doi.org/10.1128/JB.00557-19.

Editor William Margolin, McGovern Medical School

Address correspondence to Matthew A. B. Baker, matthew.baker@unsw.edu.au.

Accepted manuscript posted online 7 October 2019
Published 15 January 2020

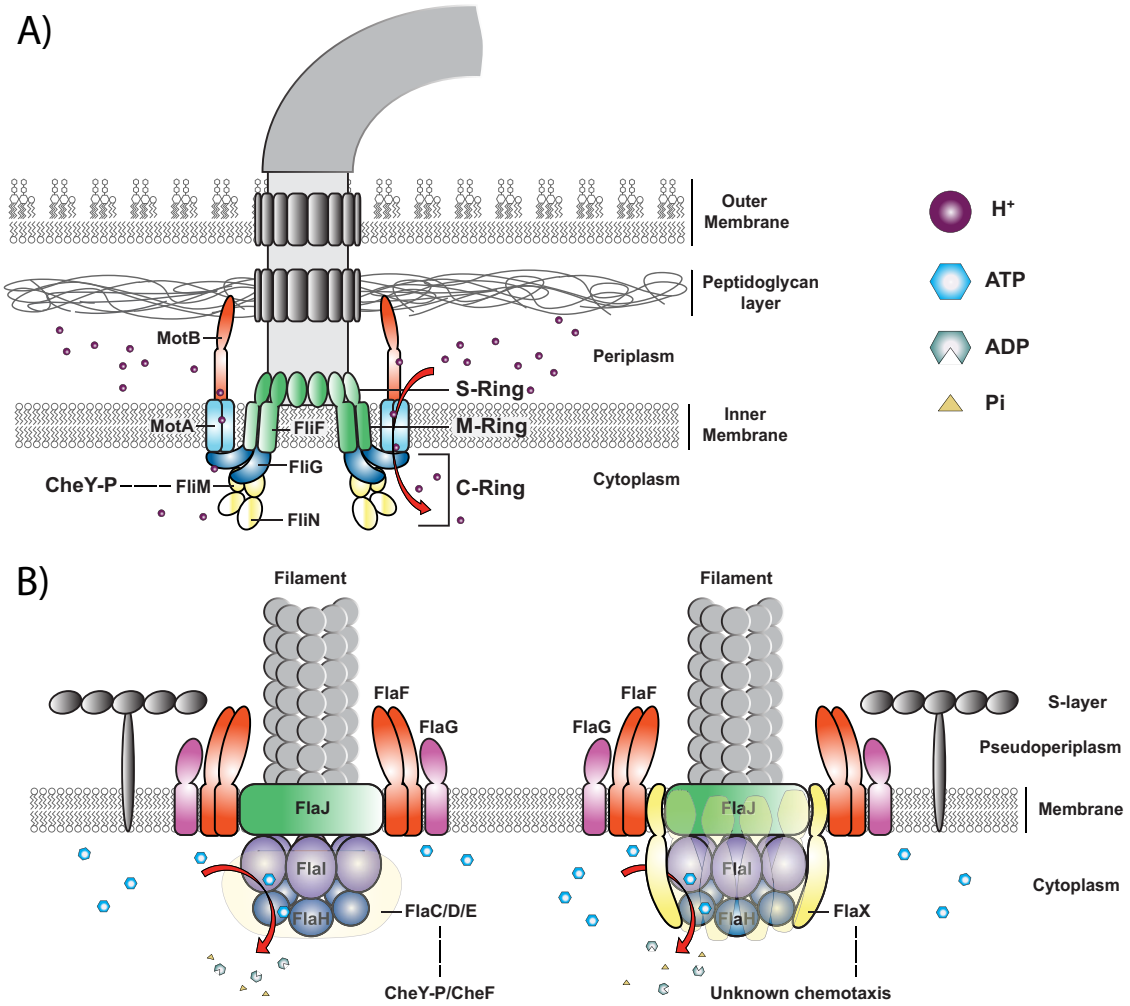

FIG 1 Schematic structures of the bacterial flagellar motor and archaeal motor. (A) The core of the flagellar motor is composed of the switch complex, containing FliG, FliM, and FliN, which forms an ~45-nm-diameter C-ring, and the stator complex, a heterodimer of MotA and MotB. Torque is generated by a proton influx through the stator complex, which triggers interactions between MotA and FliG. Directional switching occurs via interaction of the chemotaxis protein CheY-P and FliM in the switch complex, which in turn moderates interactions between FliM and FliG and between FliG and MotA. (B) Archaellins FlaJ, FlaI, FlaH, FlaF, and FlaG are conserved in the euryarchaeal (left) and crenarchaeal (right) archaella. FlaJ, FlaI, and FlaH form the archaellum core and are involved in assembly and torque. FlaJ is known to be membrane bound, buts its structure is unknown. FlaI ATPase assembles as a hexamer and interacts with the FlaH ATPase regulator. Torque occurs through hydrolysis of ATP via the assembled FlaI and FlaJ, but the exact mechanism is unknown. FlaF is postulated to anchor the archaellum to the S-layer, similar to MotB conferring motor and cell surface stability by anchoring to the peptidoglycan layer. The structure and function of FlaG are unknown. In the *Euryarchaeota*, FlaC, FlaD, and FlaE form the switch complex. The structural interactions of these archaellins are unknown, but these proteins are postulated to encircle FlaI and FlaH. Directional switching occurs through the interaction of CheY-P/CheF with FlaC, FlaD, and FlaE. In the *Crenarchaeota*, FlaX assembles as an ~30-nm-diameter ring around FlaJ, FlaI, and FlaH. FlaX has homology to chemotaxis proteins. However, the chemotaxis machinery employed is unknown.

factors that govern ion selectivity of the stators and their evolutionary relationship to other ion-coupling-dependent proteins.

STRUCTURE

The structure of the bacterial flagellar motor. Although an intact BFM in *E. coli* contains 22 different proteins, only five are directly involved in rotation and direction switching. These include three proteins in the rotor, FliG, FliM, and FliN, and two proteins, MotA and MotB, forming the MotAB stator complex (Fig. 1). Different stator complexes, such as PomAB, MotCD, and MotPS, have been found in other species (8). Energy for torque generation comes from an influx of cations across the plasma membrane, through the stator complex, driven by the electrochemical gradient, which

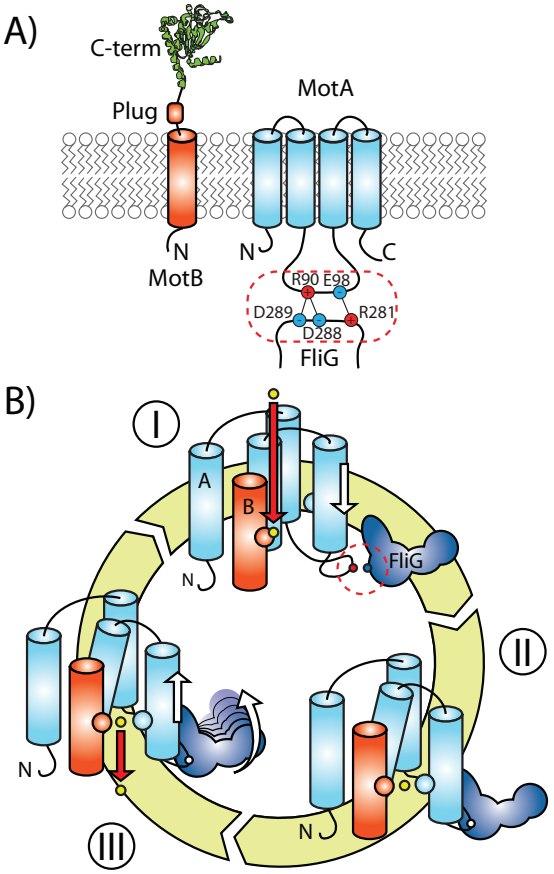

FIG 2 Topology and ion transport mechanism of the stator. (A) Schematic showing the topology of stator components MotA and MotB (monomers) also shared by PomA/PomB. Each MotA contains 4 TM helices arranged in a bundle, and the cytoplasmic loop between TM2 and TM3 displays the charged amino acid residues interacting with FliG (dashed box). Residues interacting at the MotA-FliG interface include R90/D288-D289 and E98/R281 (data from reference 10). MotB displays a single TM helix followed by a plug domain and an OmpA-like PG-anchoring domain at its C terminus. PDB identifier, 2ZVY (105). See also reference 40. (B) Schematic of the mechanochemical gating cycle of the stator. (I) When the cation (yellow circle) binds to aspartate on subunit B (red circle), this triggers a conformational change in subunit A which promotes its interaction with FliG (dashed circle). (II) The rearrangement of subunit A perturbs the ion-binding site by the action of additional side chains in the pore (blue circle), destabilizing the interaction with Asp. (III) After the release of the cation into the cytoplasm, TM3 and TM4 return to their original position while producing torque at the interface with FliG. Figure adapted from *Scientific Reports* (90).

is subsequently converted into mechanical rotation by a rotor substructure known as the switch complex. The switch complex is comprised of dozens of copies of FliG, FliM, and FliN, which form a large bell-like structure ~45 nm in diameter (the C-ring) which is responsible for torque generation, motor reversal, and regulation of rotation speed (9). Charged residues on or around a single helix in the C-terminal domain of FliG interact with at least two residues on the stator protein MotA to generate torque. However, the most significant interactions for torque occur between FliG-R298/MotA-E98 and FliG-D289/MotA-R90 (Fig. 2A) (10, 11). Motor reversal from the counterclockwise (CCW) direction to the clockwise (CW) direction is mediated by the binding between the phosphorylated form of CheY (CheY-P) and FliM (12–14). Binding of CheY-P to FliM triggers a structural change in FliM which in turn moderates interaction of FliG with the MotAB stator complex (15, 16).

The structure of the archaeal flagellum (archaellum). Overall, the archaellum is a rotary device powered by ATP hydrolysis that is structurally similar to the bacterial type IV pili (Fig. 1). The archaellum is composed of 7 to 15 proteins (archaellins), depending on species, which are homologous to bacterial type IV pilus proteins and which form

the general assembly machinery and motor complex (6). Unlike bacterial type IV pili that extend and retract, archaeal filaments rotate like flagellar filaments (17).

Of core importance to archaellum function is FlaI, a cytosolic ATPase enzyme responsible for archaellum assembly and motility (18, 19). FlaI, along with FlaJ and FlaH, forms the main motor structure in the AFM (Fig. 1B). The membrane-bound platform protein FlaJ interacts with the N-terminal domain of FlaI, and a regulator protein, FlaH, interacts with the C-terminal domain of FlaI and regulates the ATPase activity of FlaI (19–21). ATP binding and hydrolysis likely drive the switch between the open and closed conformation and rotation of the FlaI hexamer, which assembles and rotates the archaellum (19).

Most recently, functional studies on rotating archaella in *H. salinarum* (22, 23) have replicated similar measurements that had been executed earlier on the BFM using optical trapping and interferometry. These measurements have led to the current estimation for the number of ATP molecules consumed per revolution to be 6 ATPs (22).

The core FlaJ, FlaI, and FlaH motor complex is conserved across archaea. Other conserved archaellins essential for function include the membrane proteins FlaF and FlaG. The exact FlaG function is unknown. FlaF binds as a dimer to S-layer protein and anchors the archaellum in the cell envelope (24). This enables FlaF to serve as a stator and also acts to prevent membrane rupture during archaellum filament rotation. This function is similar to MotB anchoring the MotAB stator of the BFM to the peptidoglycan layer.

(i) Torque generation in archaea. In the *Euryarchaeota*, the switch complex consists of FlaC, FlaD, and FlaE (6) and is postulated to wrap around FlaI and FlaH as a cytosolic ring (Fig. 1B). However, the structural complex formed by FlaC, FlaD, and FlaE and their interaction with FlaI and FlaH are currently unknown (25). *Crenarchaeota* do not contain FlaC, FlaD, or FlaE but contain FlaX, which has a transmembrane N-terminal domain and a cytoplasmic C-terminal domain. The C-terminal domain of FlaX forms a 30-nm-diameter oligomer ring that possibly serves as the assembly scaffold for the *Crenarchaeota* motor complex (26). FlaX interacts with both FlaI (26) and FlaH (27). The FlaX ring encases both the FlaI hexamer and a ring of FlaH proteins, and the N-terminal domain of FlaX is also thought to encase FlaJ embedded in the membrane (27).

(ii) Commonality in microbial chemotaxis. The core genes of the bacterial chemotaxis machinery are conserved in the *Euryarchaeota* (28, 29). In fact, the change of rotational direction in the archaella of *H. salinarum* and *H. volcanii* is also mediated by CheY-P (30, 31). However, in the *Euryarchaeota*, CheY-P complexes with an adaptor protein, CheF, and CheF is what binds to the switch complex FlaC/D/E (30). This chemotaxis system is not found in the *Crenarchaeota*, and while FlaX has similarities to methyl-accepting chemotaxis proteins (32), the type of chemotaxis employed, and whether rotation switching occurs, remains to be shown. However, the common use of rotary motility for microbial locomotion, via very different structural, functional, and energetic pathways, is an excellent case study in convergent evolution, particularly given the conservation of CheY. This conservation of chemotactic machinery could imply that the infrastructure for chemotaxis arose once and was subsequently shared by horizontal gene transfer (HGT). However, how separate motors adapted to respond to these sensing pathways is unknown.

STATORS

The stators are where the motor transduces chemical energy from ion transit into mechanical force, and they are also the site of ion selectivity in the BFM (1). Stator complexes mainly include H^+-coupled MotAB and MotCD and Na^+-coupled PomAB and MotPS (4), but complexes coupling K^+, Rb^+, Mg^{2+}, and Ca^{2+} have also been recently discovered (33, 34). Further stator proteins exist whose primary function is to stabilize stator complexes. In *Vibrio alginolyticus*, MotXY anchors PomAB in the motor (35), and in *Sinorhizobium meliloti*, MotE maintains the stability of MotC, which in turn stabilizes the MotAB complex (36, 37).

The functional stators in the majority of the BFM are motor-associated transmem-

brane (TM) complexes made up of A and B subunits—with a stoichiometry of A(4)B(2). These form an ion channel spanning the periplasmic space and the cytoplasm. Two transmembrane regions of MotA (A-TM3 and A-TM4 [Fig. 2]) form the ion-binding channel with subunit B, with one of the remaining TM regions (A-TM2) forming one membrane anchor of the cytoplasmic loop and the other (A-TM1) having an unconfirmed function (38).

Association of the entire stator complex with the motor is accompanied by conformational changes mediated by electrostatic interactions with FliG (39, 40). Simultaneously with motor association, the stator complex attaches to the peptidoglycan layer via an OmpA-like binding domain (41–43). When this association is complete, a plug domain in the B subunit opens to allow ion influx and selectively transports cations from the periplasmic space into the cytoplasm (44).

Stator complexes likely function as a loosely coupled Brownian ratchet, where the stators can execute power strokes on the rotor driven by either one or two energizing ions (39, 45). Conformational changes in MotA are induced by ion binding in the TM region of MotB. Ion flow is obstructed by the essential aspartate residue D32 in MotB, at which point it has been proposed that protonation of D32 induces a bend in A-TM3 which is then transmitted via the A-cytoplasmic loop to FliG to allow final passage of the ion into the cytoplasm (Fig. 2B) (46). Molecular dynamics modeling suggests that hydrogen bonding between protonated D32 in MotB and D170 in A-TM3 induces the conformational change which pivots around P173 in A-TM3 (47).

Loss-of-function mutants of MotB that cause a misalignment of the stator relative to FliG could be rescued by mutations in MotA at the pore interface to restore proton conduction, although with some loss in motor performance (48, 49). Furthermore, the efficiency of the force transfer from the stator to FliG appears to depend on the presence of prolines (P173 and P222) at the cytoplasmic end of MotA TM helices that presumably restrict the motion of the stator during the cascade of conformational changes to optimize the power stroke. In fact, the replacement of an arginine residue with a proline (R109P) in the α-helix connecting the transmembrane and peptidoglycan binding domains in a nonfunctional chimeric PotB construct, consisting of a C-terminal PomB and N-terminal MotB, restored Na^+ conductivity in the chimera by conferring a proper arrangement of transmembrane helices (50). These examples highlight how the structural requirements for coupling ion passage through the stator to force generation can be met by several amino acid configurations displayed from either pore subunit.

Binding to the conserved aspartate residue (D32) within the TM region of the B subunit causes conformational changes that drive torque generation (39, 51). In *V. alginolyticus*, seven residues in PomA and six residues in FliG contribute to torque generation, with the interaction between PomA-E97 and FliG-K284 being critical for function (40). The equivalent conserved glutamate residue, E96, in *Aquifex aeolicus* MotA, along with R88, is important in the function of the hyperthermophile's flagellar motor (40, 52–54). These residues are exposed on the cytoplasmic loop surface between A-TM2 and A-TM3 which forms the interface with FliG. Chimeras of *A. aeolicus* and *E. coli* stator proteins are functional in *E. coli* flagellar motors, suggesting that the interaction between the A subunit and the rotor is highly conserved and ancient (55). However, there are differences between *E. coli* MotA and *V. alginolyticus* PomA in their interactions with FliG, as the cytoplasmic loop of PomA has more charged residue interactions with FliG than the loop of MotA (40).

SELECTIVITY

The cations selected by the stator complex are most commonly protons or sodium ions, as seen in enteric bacteria and *Vibrio* spp. (1). However, stators that utilize other ions of the alkali metal group have been discovered, such as rubidium and potassium in alkaliphilic *Bacillus* (34). Some bacterial species even have the ability to couple multiple ions via the use of multiple sets of stator genes encoding different stator proteins, e.g., *Bacillus subtilis* and *Shewanella oneidensis* (56, 57), or single, dual-purpose complexes such as in *Pseudomonas aeruginosa* and alkaliphilic *Bacillus* (34, 58). Dual ion

use can be introduced into single-use stators with mutations in the ion-binding transmembrane region of the B unit, as seen in *Bacillus subtilis* (59). A *Paenibacillus* species has been found that couples divalent magnesium and calcium ions, which are abundant in its environment, for motility, providing the possibility of flagellar rotation powered by multivalent ions (33).

Attempts to obtain information about the TM regions of MotA and MotB have been hindered by the difficulty of generating crystals (here in *Helicobacter pylori*) (42). Recently, a combination of electron microscopy single-particle imaging in *A. aeolicus* (60); molecular dynamics (47); and small-angle X-ray scattering (SAXS) in *H. pylori*, *Salmonella enterica*, and *V. alginolyticus* (61, 62) has refined models for MotA and MotB, but an atomic structure, perhaps via improved single-particle cryo-electron microscopy (cryo-EM), is yet to be determined.

Filter. Molecular dynamics simulations of the ion channel region have proffered size exclusion as a mechanism for ion selectivity (47). The radius of the ion channel created by MotB residues 19 to 54 was predicted to be 1.0 to 2.3 Å in a nonprotonated state, with the narrowest point occurring at L46. Protonation of critical residue D32 expands the channel near the cytoplasm and the periplasm to promote entry and ejection of the translocating ion, but the channel remains narrow at L46 to maintain selectivity. Increases in radius of the ion channel typically improve sodium flux over proton flux as seen in Na^+-coupled ATP synthases (63). Thus, ion selectivity in the stator complex does not appear to rely solely on size exclusion, nor to be controlled by a single residue. However, in *Vibrio cholerae*, PomB-S26, located on the same face of the B-TM helix as the conserved aspartate D23, is known to be important for optimal swimming and is thought to disrupt the hydration shell of Na^+, allowing the ion to move through a constriction in the channel (64).

The *E. coli* MotAB complex and the *V. alginolyticus* PomAB complex are the best-characterized H^+- and Na^+-coupled stators, respectively. A chimeric B unit, PotB, consisting of the TM helix and cytoplasmic domain of *V. alginolyticus* PomB (residues 1 to 50) and the peptidoglycan-binding (PGB) domain and periplasmic linker of *E. coli* MotB (residues 59 to 300), has been used extensively to study underenergized motors at low sodium concentration in *E. coli* (1).

PotB forms a chimeric stator complex with PomA ($PomA_4PotB_2$) and restores motility in *E. coli* Δ*motAB* as an Na^+-coupled PomA/PotB stator complex (65). In the PotB chimera, the ion channel is made exclusively of the *V. alginolyticus* PomA and PotB TM region, with the N-terminal *E. coli* component of the B subunit allowing the complex to bind to the peptidoglycan layer. This further verifies that B-TM, A-TM3, and A-TM4 determine ion selectivity, as anticipated by previous research with stator chimeras in *Rhodobacter sphaeroides* and *V. alginolyticus* (65).

EVOLUTION

The BFM shares core structural components with the pathogenic injectisome of proteobacteria, the nonflagellar type III secretion system (T3SS) (66). It is likely that the T3SS evolved through the exaptation of genes of the BFM, as evidenced by modern phylogenies of flagellar and nonflagellar T3SS (67). The evolutionary primacy of the BFM is also supported by the T3SS's constrained existence in newer bacterial phyla relative to the broader spread of flagellar motors (68). The oldest forms of the BFM reside in early-branched hyperthermophilic bacteria (55). By looking at B subunit chimeras of *A. aeolicus* and *E. coli* in *E. coli*, we can understand which interactions between stators and motors have been conserved. A chimera combining the TM region of *A. aeolicus* MotB and the PGB domain of *E. coli* MotB forms a functional stator complex with *A. aeolicus* MotA in *E. coli*. The interaction between *A. aeolicus* stators and *E. coli* rotors suggests that the interactions between FliG and MotA, which drive torque generation in the BFM (Fig. 1), must be highly conserved, even among phylogenetically distant taxa.

Of the ~50 gene products necessary to produce the BFM, perhaps as few as two proteins both are indispensable to function in all known varieties of motors and do not

share a known sequence homology with another extant protein (69). Therefore, far from being irreducibly complex, the BFM contains an overwhelmingly large amount of modular, bifunctional, and noncritical mass that points to a common ancestral beginning.

Origins of stators. MotA and MotB share sequence homology with other proton-coupled TM transport systems. The Tol-Pal system in *E. coli* is implicated in membrane stability and protein transport, and it depends on the proton motive force (PMF) for function (70). This system consists of TolQ, a polytopic cytoplasmic membrane-spanning protein analogous to MotA, and component TolR, a MotB analogue, that transmits a signal to TolA in active colicin uptake. TolQR shares TM structural and functional homology with MotAB, as does ExbBD of the TonB system (71). ExbBD uses the PMF to energize transport of siderophores and vitamin B_{12} in Gram-negative bacteria. In ExbD, a homologue of MotB, a mutation of a conserved aspartate residue in the TM domain abolishes the function of the complex (72), as it does when the conserved aspartate D32 in MotB is mutated.

There is also evidence of horizontal gene transfer (HGT) of flagellar motor and stator genes occurring between bacterial taxa; the alphaproteobacterium *R. sphaeroides* contains a second set of flagellar motor genes acquired through HGT from a gammaproteobacterium (73), and *Rhodospirillum centenum* acquired its second set of stator genes from a *Vibrio* species (74). *S. oneidensis*, the only member of its genus to live in freshwater, is predicted to have received its H^+-coupled MotAB stator from a sympatric *Aeromonas* species, whereas its Na^+-coupled PomAB stator is homologous to marine members of its genus (75). Takekawa et al. (55) demonstrated that the hyperthermophilic *A. aeolicus* MotA and MotB conduct Na^+, suggesting that filament rotation in ancient bacteria was driven by Na^+, as these bacteria are thought to possess some of the first motor proteins to have evolved. Furthermore, due to the low sequence similarity between Na^+- and H^+-coupled stators in bacteria that have both types of stator, it was suggested that *Aquifex* and *Thermotoga* are common recipients of ancestral sodium-coupled flagellar stator genes (55), as both genera are predominantly hyperthermophilic and share significant genome homology with archaea (76). It is possible that *A. aeolicus* shares a MotB lineage with *Epsilonproteobacteria* (77), a class of bacteria with members that colonize hydrothermal vents typical of *Aquificae*, *Thermotogae*, and other early-branched bacterial and archaeal lineages.

Although phylogenetic data do not support the assumption that Na^+-coupled stators arose first, the assumption that ancestral microbes in high-salt environments would be powered by sodium motive force aligns with contemporary theories for ancient membrane bioenergetics (78). Na^+ coupling is thought to have arisen before H^+ coupling in F_1F_o-ATP synthetases (79). Generally, the hypothesis that Na^+ selection predates H^+ selection in TM protein complexes is well supported (80) but only circumstantially supported in stators by looking at the ion-coupling preferences of contemporary bacteria and comparing this to their evolutionary age (55).

Insights from other bacterial ion transporters. The proton transport mechanism through the stator complex is more akin to ion transporters than typical ion channels. For ion channels, opening produces a continuous water-filled pore through which water and ions pass, often in single file through the narrowest region, while in transporters one or a few ions are transferred across the bilayer as a result of a series of dedicated conformational changes in the protein (81). This makes ion transporters orders of magnitude slower than channels at moving ions. Theoretical calculations of ionic flow rates estimate $\sim 2 \times 10^5$ H^+/s through an *E. coli* stator, whereas the observed rate for voltage-gated sodium channels is on the order of 10^7 Na^+/s (82, 83). Similarly to the N-type inactivation observed in voltage-gated sodium channels (84), the flow of ions through the MotAB stator complex can be inactivated by the action of the plug domain of MotB (44). In the BFM, this inactivation is maintained before the stator complex assembles onto the rotor to prevent leakage of ions prior to motor assembly rather than to cease flow after sustained ion conduction, as in other channels. Activa-

tion of the stator depends on binding of the C-terminal OmpA-like domain of MotB to the peptidoglycan layer (85).

The rate of proton flux at the MotA/B interface is limited by the rate of conformational change that is induced via the binding and release of H^+ to the aspartic acid residue D32 in the stator (86, 87). As per an ion transporter, this mechanochemical process relies on the sequential binding of H^+ to an acidic amino acid (e.g., D32 in *E. coli* MotB), followed by a conformational change and the subsequent release of H^+ from the amino acid to regenerate the proton-binding site, thus limiting the ion flux to one proton per torque-generating cycle of conformational change at each pore (~1,200 protons per revolution per motor in *Streptococcus* spp. and *E. coli*) (39, 88, 89). This mode of transport appears to be conserved in Na^+-powered stators, which employ additional polar amino acid residues along the pore to accommodate the binding and release of sodium ions (90).

It has been speculated that substantial transmembrane helical movements are required for ion channels to transition between open and closed states (91). Such movements might be inefficient or infeasible in a single protein with an ion conduction pathway through its center in comparison with the interface of separate subunits. Thus, ion conduction at protein interfaces possibly provides an essential flexible pathway that enables rapid conformational changes (91).

Helix swiveling has been proposed as a critical consequence of aspartate protonation during H^+ transport in the F_o subunit of the *E. coli* ATP synthase (92). A similar mechanism might be involved in the force generation step in the BFM stator (90). In contrast to the BFM, however, H^+ selectivity in the bacterial ATP synthases has been suggested to be determined by the c-ring rotor of F_o rather than the interfaces in the stator *a* subunit (93). The binding of H^+ to R61 on the c-ring directly mediates a 36° rotation of the c-ring by modulation of the electrostatic interactions at the stator-rotor interface and the twisting of the protonated helix (93).

Other homologous complexes for the stator exist in prokaryotes that exploit PMF to couple a "power stroke" or conformational change to various outputs (Fig. 3). The TonB-ExbB-ExbD complex plays an essential role in siderophore acquisition in *E. coli*, transducing PMF into translocation (94, 95). The TolQ-TolR stator complex of *E. coli* is recruited to cell division sites, where it is coupled to proteins dedicated to maintaining the integrity of the outer membrane (96). Last, the AglR/Q stator of *Myxococcus xanthus* drives a distinct bacterial motor involved in gliding motility (97). In flagellar stators, the selectivity for protons, and presumably for sodium ions, appears to be dependent on interfacial residues from both A and B subunits, suggesting a coevolutionary linkage underlying the mechanism of PMF-driven torque generation. This may have been relevant for the adaptation of motility machinery after the oxygenation of the atmosphere in ancient times, when the enzymes involved in membrane bioenergetics, to maintain the Na^+/K^+ disequilibrium across the membrane, gradually implemented Na^+/H^+ transport mechanisms (80, 98). With the concomitant evolution of membrane lipids to cope with the new environment (99), prokaryotic membranes became largely impermeable to both sodium ions and protons, and proton-dependent bioenergetics became prevalent (78).

CONCLUSIONS

The high structural diversity of the flagellar motor complex across contemporary bacterial taxa and recent improvements in cryotomography have enabled the first predictions of the quaternary structure of the ancestral complex. In particular, recent papers have revealed the extent of contemporary diversity (100–103)—and have used high-resolution imaging of larger rotors in species such as *Borrelia burgdorferi* to elucidate torque-generating interactions between the stator and rotor (104). Thus, the discovery of these new BFM basal-body structures has shed new light on the motor, even in long-studied model organisms. The inability to resolve an atomic structure of the transmembrane domains of the stator complex, however, means that we do not yet

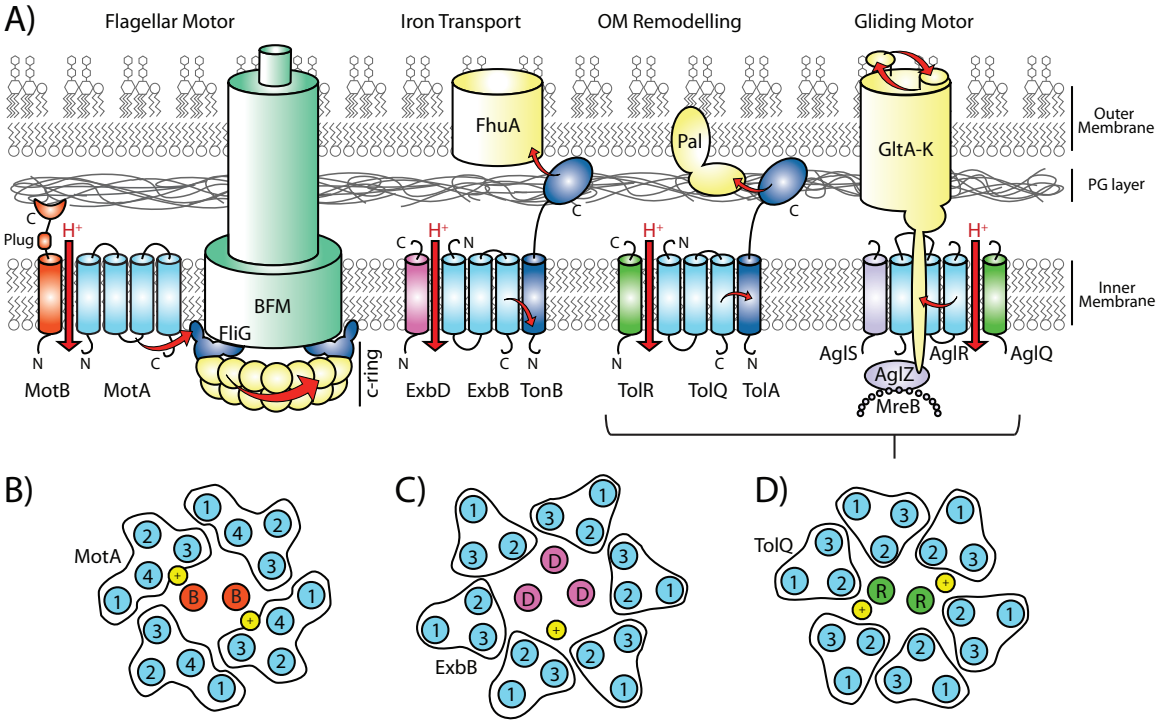

FIG 3 PMF-coupled systems in prokaryotes. (A) Cartoon diagram of prokaryotic membrane machinery employing stator homologues to couple PMF to various biological outputs. Proton transport at the stator subunit interface (straight downward arrow) generates a mechanical interaction with downstream effectors (curved red arrow) to provide torque to the flagellar motor (MotA/MotB), to activate iron transport (ExbB/ExbD), to promote outer membrane remodeling (TolQ/TolR), or to drive gliding propulsion (AglQ/AglR/AglS) in each system, respectively. All complexes are shown with 1:1 stoichiometries. The stoichiometry of MotAB is 4:2, that of ExbBD is 6:3 (95), that of TolQR is 6:2 (96), and that of AglQR is not known, albeit speculated to be homologous to TolQR (97). (Figure modified from reference 106 with permission of the publisher.) (B to D) Schematic view of the stators from the extracellular side. (B) The BFM stator subunit A contains 4 TM helices, while subunit B contains only a single TM. The two B subunit TMs and TM3 and TM4 of two A subunits assemble to form two ion-conducting pathways (yellow area). (C) ExbB contains 3 TM helices per subunit and assembles with ExbD to form a single ion conduction pathway per stator. (D) TolQ/AglR is thought to contain 3 TMs per subunit and to assemble with TolR/AglQ in a 6:2 ratio to form two proton-conducting pathways.

have a full understanding of the physical processes behind torque generation and ion selectivity.

Further structural understanding of the stators may shed light on the conformational rearrangements accompanying torque generation and the pore profile and residues involved in ion selectivity. New experiments in directed and experimental evolution will inform the molecular basis of evolution and adaptation in complex multicomponent systems.

ACKNOWLEDGMENTS

M. M. Tanaka is supported by Australian Research Council Future Fellowship FT140100398. M. A. B. Baker is supported by Australian Research Council Discovery Project DP190100497 and a CSIRO Future Platform in Synthetic Biology 2018 Project Grant.

REFERENCES

1. Sowa Y, Berry RM. 2008. Bacterial flagellar motor. Q Rev Biophys 41:103–132. https://doi.org/10.1017/S0033583508004691.
2. Mitchell JG, Kogure K. 2006. Bacterial motility: links to the environment and a driving force for microbial physics. FEMS Microbiol Ecol 55:3–16. https://doi.org/10.1111/j.1574-6941.2005.00003.x.
3. Son K, Brumley DR, Stocker R. 2015. Live from under the lens: exploring microbial motility with dynamic imaging and microfluidics. Nat Rev Microbiol 13:761–775. https://doi.org/10.1038/nrmicro3567.
4. Thormann KM, Paulick A. 2010. Tuning the flagellar motor. Microbiology 156:1275–1283. https://doi.org/10.1099/mic.0.029595-0.
5. Pion M, Bshary R, Bindschedler S, Filippidou S, Wick LY, Job D, Junier P. 2013. Gains of bacterial flagellar motility in a fungal world. Appl Environ Microbiol 79:6862–6867. https://doi.org/10.1128/AEM.01393-13.
6. Albers S-V, Jarrell KF. 2018. The archaellum: an update on the unique archaeal motility structure. Trends Microbiol 26:351–362. https://doi.org/10.1016/j.tim.2018.01.004.

7. Albers S-V, Jarrell KF. 2015. The archaellum: how Archaea swim. Front Microbiol 6:23. https://doi.org/10.3389/fmicb.2015.00023.
8. Nakamura S, Minamino T. 2019. Flagella-driven motility of bacteria. Biomolecules 9:E279. https://doi.org/10.3390/biom9070279.
9. Xue R, Ma Q, Baker MAB, Bai F. 2015. A delicate nanoscale motor made by nature—the bacterial flagellar motor. Adv Sci (Weinh) 2:1500129. https://doi.org/10.1002/advs.201500129.
10. Zhou J, Sharp LL, Tang HL, Lloyd SA, Billings S, Braun TF, Blair DF. 1998. Function of protonatable residues in the flagellar motor of *Escherichia coli*: a critical role for Asp 32 of MotB. J Bacteriol 180:2729–2735.
11. Stock D, Namba K, Lee LK. 2012. Nanorotors and self-assembling macromolecular machines: the torque ring of the bacterial flagellar motor. Curr Opin Biotechnol 23:545–554. https://doi.org/10.1016/j.copbio.2012.01.008.
12. Bren A, Eisenbach M. 1998. The N terminus of the flagellar switch protein, FliM, is the binding domain for the chemotactic response regulator, CheY. J Mol Biol 278:507–514. https://doi.org/10.1006/jmbi.1998.1730.
13. Fukuoka H, Sagawa T, Inoue Y, Takahashi H, Ishijima A. 2014. Direct imaging of intracellular signaling components that regulate bacterial chemotaxis. Sci Signal 7:ra32. https://doi.org/10.1126/scisignal.2004963.
14. Welch M, Oosawa K, Aizawa S, Eisenbach M. 1993. Phosphorylation-dependent binding of a signal molecule to the flagellar switch of bacteria. Proc Natl Acad Sci U S A 90:8787–8791. https://doi.org/10.1073/pnas.90.19.8787.
15. Lee LK, Ginsburg MA, Crovace C, Donohoe M, Stock D. 2010. Structure of the torque ring of the flagellar motor and the molecular basis for rotational switching. Nature 466:996–1000. https://doi.org/10.1038/nature09300.
16. Toker AS, Macnab RM. 1997. Distinct regions of bacterial flagellar switch protein FliM interact with FliG, FliN and CheY. J Mol Biol 273:623–634. https://doi.org/10.1006/jmbi.1997.1335.
17. Shahapure R, Driessen RPC, Haurat MF, Albers S-V, Dame RTh. 2014. The archaellum: a rotating type IV pilus. Mol Microbiol 91:716–723. https://doi.org/10.1111/mmi.12486.
18. Ghosh A, Hartung S, van der Does C, Tainer JA, Albers S-V. 2011. Archaeal flagellar ATPase motor shows ATP-dependent hexameric assembly and activity stimulation by specific lipid binding. Biochem J 437:43–52. https://doi.org/10.1042/BJ20110410.
19. Reindl S, Ghosh A, Williams GJ, Lassak K, Neiner T, Henche A-L, Albers S-V, Tainer JA. 2013. Insights on FlaI functions in archaeal motor assembly and motility from structures, conformations and genetics. Mol Cell 49:1069–1082. https://doi.org/10.1016/j.molcel.2013.01.014.
20. Banerjee A, Neiner T, Tripp P, Albers S-V. 2013. Insights into subunit interactions in the *Sulfolobus acidocaldarius* archaellum cytoplasmic complex. FEBS J 280:6141–6149. https://doi.org/10.1111/febs.12534.
21. Chaudhury P, van der Does C, Albers S-V. 2018. Characterization of the ATPase FlaI of the motor complex of the *Pyrococcus furiosus* archaellum and its interactions between the ATP-binding protein FlaH. PeerJ 6:e4984. https://doi.org/10.7717/peerj.4984.
22. Iwata S, Kinosita Y, Uchida N, Nakane D, Nishizaka T. 2019. Motor torque measurement of *Halobacterium salinarum* archaellar suggests a general model for ATP-driven rotary motors. Commun Biol 2:199. https://doi.org/10.1038/s42003-019-0422-6.
23. Kinosita Y, Uchida N, Nakane D, Nishizaka T. 2016. Direct observation of rotation and steps of the archaellum in the swimming halophilic archaeon *Halobacterium salinarum*. Nat Microbiol 1:16148. https://doi.org/10.1038/nmicrobiol.2016.148.
24. Banerjee A, Tsai C-L, Chaudhury P, Tripp P, Arvai AS, Ishida JP, Tainer JA, Albers S-V. 2015. FlaF is a β-sandwich protein that anchors the archaellum in the archaeal cell envelope by binding the S-layer protein. Structure 23:863–872. https://doi.org/10.1016/j.str.2015.03.001.
25. Daum B, Vonck J, Bellack A, Chaudhury P, Reichelt R, Albers S-V, Rachel R, Kühlbrandt W. 2017. Structure and in situ organisation of the *Pyrococcus furiosus* archaellum machinery. Elife 6:e27470. https://doi.org/10.7554/eLife.27470.
26. Banerjee A, Ghosh A, Mills DJ, Kahnt J, Vonck J, Albers S-V. 2012. FlaX, a unique component of the crenarchaeal archaellum, forms oligomeric ring-shaped structures and interacts with the motor ATPase FlaI. J Biol Chem 287:43322–43330. https://doi.org/10.1074/jbc.M112.414383.
27. Chaudhury P, Neiner T, D'Imprima E, Banerjee A, Reindl S, Ghosh A, Arvai AS, Mills DJ, van der Does C, Tainer JA, Vonck J, Albers S-V. 2016. The nucleotide-dependent interaction of FlaH and FlaI is essential for assembly and function of the archaellum motor. Mol Microbiol 99:674–685. https://doi.org/10.1111/mmi.13260.
28. Briegel A, Ortega DR, Huang AN, Oikonomou CM, Gunsalus RP, Jensen GJ. 2015. Structural conservation of chemotaxis machinery across archaea and bacteria. Environ Microbiol Rep 7:414–419. https://doi.org/10.1111/1758-2229.12265.
29. Wuichet K, Cantwell BJ, Zhulin IB. 2010. Evolution and phyletic distribution of two-component signal transduction systems. Curr Opin Microbiol 13:219–225. https://doi.org/10.1016/j.mib.2009.12.011.
30. Quax TEF, Altegoer F, Rossi F, Li Z, Rodriguez-Franco M, Kraus F, Bange G, Albers S-V. 2018. Structure and function of the archaeal response regulator CheY. Proc Natl Acad Sci U S A 115:E1259–E1268. https://doi.org/10.1073/pnas.1716661115.
31. Schlesner M, Miller A, Besir H, Aivaliotis M, Streif J, Scheffer B, Siedler F, Oesterhelt D. 2012. The protein interaction network of a taxis signal transduction system in a halophilic archaeon. BMC Microbiol 12:272. https://doi.org/10.1186/1471-2180-12-272.
32. Ghosh A, Albers S-V. 2011. Assembly and function of the archaeal flagellum. Biochem Soc Trans 39:64–69. https://doi.org/10.1042/BST0390064.
33. Imazawa R, Takahashi Y, Aoki W, Sano M, Ito M. 2016. A novel type bacterial flagellar motor that can use divalent cations as a coupling ion. Sci Rep 6:19773. https://doi.org/10.1038/srep19773.
34. Terahara N, Sano M, Ito M. 2012. A *Bacillus* flagellar motor that can use both Na^+ and K^+ as a coupling ion is converted by a single mutation to use only Na^+. PLoS One 7:e46248. https://doi.org/10.1371/journal.pone.0046248.
35. Terashima H, Li N, Sakuma M, Koike M, Kojima S, Homma M, Imada K. 2013. Insight into the assembly mechanism in the supramolecular rings of the sodium-driven *Vibrio* flagellar motor from the structure of FlgT. Proc Natl Acad Sci U S A 110:6133–6138. https://doi.org/10.1073/pnas.1222655110.
36. Eggenhofer E, Haslbeck M, Scharf B. 2004. MotE serves as a new chaperone specific for the periplasmic motility protein, MotC, in *Sinorhizobium meliloti*. Mol Microbiol 52:701–712. https://doi.org/10.1111/j.1365-2958.2004.04022.x.
37. Platzer J, Sterr W, Hausmann M, Schmitt R. 1997. Three genes of a motility operon and their role in flagellar rotary speed variation in *Rhizobium meliloti*. J Bacteriol 179:6391–6399. https://doi.org/10.1128/jb.179.20.6391-6399.1997.
38. Braun TF, Al-Mawsawi LQ, Kojima S, Blair DF. 2004. Arrangement of core membrane segments in the MotA/MotB proton-channel complex of *Escherichia coli*. Biochemistry 43:35–45. https://doi.org/10.1021/bi035406d.
39. Kojima S, Blair DF. 2001. Conformational change in the stator of the bacterial flagellar motor. Biochemistry 40:13041–13050. https://doi.org/10.1021/bi011263o.
40. Takekawa N, Kojima S, Homma M. 2014. Contribution of many charged residues at the stator-rotor interface of the Na^+-driven flagellar motor to torque generation in *Vibrio alginolyticus*. J Bacteriol 196:1377–1385. https://doi.org/10.1128/JB.01392-13.
41. De Mot R, Vanderleyden J. 1994. The C-terminal sequence conservation between OmpA-related outer membrane proteins and MotB suggests a common function in both gram-positive and gram-negative bacteria, possibly in the interaction of these domains with peptidoglycan. Mol Microbiol 12:333–334. https://doi.org/10.1111/j.1365-2958.1994.tb01021.x.
42. Roujeinikova A. 2008. Crystal structure of the cell wall anchor domain of MotB, a stator component of the bacterial flagellar motor: implications for peptidoglycan recognition. Proc Natl Acad Sci U S A 105:10348–10353. https://doi.org/10.1073/pnas.0803039105.
43. Hizukuri Y, Kojima S, Homma M. 2010. Disulphide cross-linking between the stator and the bearing components in the bacterial flagellar motor. J Biochem 148:309–318. https://doi.org/10.1093/jb/mvq067.
44. Hosking ER, Vogt C, Bakker EP, Manson MD. 2006. The *Escherichia coli* MotAB proton channel unplugged. J Mol Biol 364:921–937. https://doi.org/10.1016/j.jmb.2006.09.035.
45. Boschert R, Adler FR, Blair DF. 2015. Loose coupling in the bacterial flagellar motor. Proc Natl Acad Sci U S A 112:4755–4760. https://doi.org/10.1073/pnas.1419955112.
46. Kim EA, Marian P-C, Carlquist WC, Blair DF. 2008. Membrane segment organization in the stator complex of the flagellar motor: implications for proton flow and proton-induced conformational change. Biochemistry 47:11332–11339. https://doi.org/10.1021/bi801347a.

47. Nishihara Y, Kitao A. 2015. Gate-controlled proton diffusion and protonation-induced ratchet motion in the stator of the bacterial flagellar motor. Proc Natl Acad Sci U S A 112:7737–7742. https://doi.org/10.1073/pnas.1502991112.
48. Garza AG, Harris-Haller LW, Stoebner RA, Manson MD. 1995. Motility protein interactions in the bacterial flagellar motor. Proc Natl Acad Sci U S A 92:1970–1974. https://doi.org/10.1073/pnas.92.6.1970.
49. Garza AG, Biran R, Wohlschlegel JA, Manson MD. 1996. Mutations in MotB suppressible by changes in stator or rotor components of the bacterial flagellar motor. J Mol Biol 258:270–285. https://doi.org/10.1006/jmbi.1996.0249.
50. Zhu S, Homma M, Kojima S. 2012. Intragenic suppressor of a plug deletion nonmotility mutation in PotB, a chimeric stator protein of sodium-driven flagella. J Bacteriol 194:6728–6735. https://doi.org/10.1128/JB.01132-12.
51. Sudo Y, Okada A, Suzuki D, Inoue K, Irieda H, Sakai M, Fujii M, Furutani Y, Kandori H, Homma M. 2009. Characterization of a signaling complex composed of sensory rhodopsin I and its cognate transducer protein from the eubacterium *Salinibacter ruber*. Biochemistry 48:10136–10145. https://doi.org/10.1021/bi901338d.
52. Lloyd SA, Blair DF. 1997. Charged residues of the rotor protein FliG essential for torque generation in the flagellar motor of *Escherichia coli*. J Mol Biol 266:733–744. https://doi.org/10.1006/jmbi.1996.0836.
53. Morimoto YV, Nakamura S, Kami-Ike N, Namba K, Minamino T. 2010. Charged residues in the cytoplasmic loop of MotA are required for stator assembly into the bacterial flagellar motor. Mol Microbiol 78:1117–1129. https://doi.org/10.1111/j.1365-2958.2010.07391.x.
54. Zhou J, Blair DF. 1997. Residues of the cytoplasmic domain of MotA essential for torque generation in the bacterial flagellar motor. J Mol Biol 273:428–439. https://doi.org/10.1006/jmbi.1997.1316.
55. Takekawa N, Nishiyama M, Kaneseki T, Kanai T, Atomi H, Kojima S, Homma M. 2015. Sodium-driven energy conversion for flagellar rotation of the earliest divergent hyperthermophilic bacterium. Sci Rep 5:12711. https://doi.org/10.1038/srep12711.
56. Paulick A, Koerdt A, Lassak J, Huntley S, Wilms I, Narberhaus F, Thormann KM. 2009. Two different stator systems drive a single polar flagellum in *Shewanella oneidensis* MR-1. Mol Microbiol 71:836–850. https://doi.org/10.1111/j.1365-2958.2008.06570.x.
57. Ito M, Terahara N, Fujinami S, Krulwich TA. 2005. Properties of motility in *Bacillus subtilis* powered by the H^+-coupled MotAB flagellar stator, Na^+-coupled MotPS or hybrid stators MotAS or MotPB. J Mol Biol 352:396–408. https://doi.org/10.1016/j.jmb.2005.07.030.
58. Doyle TB, Hawkins AC, McCarter LL. 2004. The complex flagellar torque generator of *Pseudomonas aeruginosa*. J Bacteriol 186:6341–6350. https://doi.org/10.1128/JB.186.19.6341-6350.2004.
59. Terahara N, Krulwich TA, Ito M. 2008. Mutations alter the sodium versus proton use of a *Bacillus clausii* flagellar motor and confer dual ion use on *Bacillus subtilis* motors. Proc Natl Acad Sci U S A 105:14359–14364. https://doi.org/10.1073/pnas.0802106105.
60. Takekawa N, Terahara N, Kato T, Gohara M, Mayanagi K, Hijikata A, Onoue Y, Kojima S, Shirai T, Namba K, Homma M. 2016. The tetrameric MotA complex as the core of the flagellar motor stator from hyperthermophilic bacterium. Sci Rep 6:31526. https://doi.org/10.1038/srep31526.
61. Andrews DA, Nesmelov YE, Wilce MC, Roujeinikova A. 2017. Structural analysis of variant of *Helicobacter pylori* MotB in its activated form, engineered as chimera of MotB and leucine zipper. Sci Rep 7:13435. https://doi.org/10.1038/s41598-017-13421-0.
62. Liew CW, Hynson RM, Ganuelas LA, Shah-Mohammadi N, Duff AP, Kojima S, Homma M, Lee LK. 2018. Solution structure analysis of the periplasmic region of bacterial flagellar motor stators by small angle X-ray scattering. Biochem Biophys Res Commun 495:1614–1619. https://doi.org/10.1016/j.bbrc.2017.11.194.
63. Krah A, Pogoryelov D, Langer JD, Bond PJ, Meier T, Faraldo-Gómez JD. 2010. Structural and energetic basis for H^+ versus Na^+ binding selectivity in ATP synthase F_o rotors. Biochim Biophys Acta 1797:763–772. https://doi.org/10.1016/j.bbabio.2010.04.014.
64. Halang P, Vorburger T, Steuber J. 2015. Serine 26 in the PomB subunit of the flagellar motor is essential for hypermotility of *Vibrio cholerae*. PLoS One 10:e0123518. https://doi.org/10.1371/journal.pone.0123518.
65. Asai Y, Kawagishi I, Sockett RE, Homma M. 2000. Coupling ion specificity of chimeras between H^+- and Na^+-driven motor proteins, MotB and PomB, in *Vibrio* polar flagella. EMBO J 19:3639–3648. https://doi.org/10.1093/emboj/19.14.3639.
66. Diepold A, Kudryashev M, Delalez NJ, Berry RM, Armitage JP. 2015. Composition, formation, and regulation of the cytosolic C-ring, a dynamic component of the type III secretion injectisome. PLoS Biol 13:e1002039. https://doi.org/10.1371/journal.pbio.1002039.
67. Abby SS, Rocha E. 2012. The non-flagellar type III secretion system evolved from the bacterial flagellum and diversified into host-cell adapted systems. PLoS Genet 8:e1002983. https://doi.org/10.1371/journal.pgen.1002983.
68. Nguyen L, Paulsen IT, Tchieu J, Hueck CJ, Saier MH. 2000. Phylogenetic analyses of the constituents of type III protein secretion systems. J Mol Microbiol Biotechnol 2:125–144.
69. Pallen MJ, Matzke NJ. 2006. From The Origin of Species to the origin of bacterial flagella. Nat Rev Microbiol 4:784–790. https://doi.org/10.1038/nrmicro1493.
70. Cascales E, Lloubès R, Sturgis JN. 2001. The TolQ-TolR proteins energize TolA and share homologies with the flagellar motor proteins MotA-MotB. Mol Microbiol 42:795–807. https://doi.org/10.1046/j.1365-2958.2001.02673.x.
71. Marmon L. 2013. Elucidating the origin of the ExbBD components of the TonB system through Bayesian inference and maximum-likelihood phylogenies. Mol Phylogenet Evol 69:674–686. https://doi.org/10.1016/j.ympev.2013.07.010.
72. Ollis AA, Manning M, Held KG, Postle K. 2009. Cytoplasmic membrane protonmotive force energizes periplasmic interactions between ExbD and TonB. Mol Microbiol 73:466–481. https://doi.org/10.1111/j.1365-2958.2009.06785.x.
73. Poggio S, Abreu-Goodger C, Fabela S, Osorio A, Dreyfus G, Vinuesa P, Camarena L. 2007. A complete set of flagellar genes acquired by horizontal transfer coexists with the endogenous flagellar system in *Rhodobacter sphaeroides*. J Bacteriol 189:3208–3216. https://doi.org/10.1128/JB.01681-06.
74. McClain J, Rollo DR, Rushing BG, Bauer CE. 2002. *Rhodospirillum centenum* utilizes separate motor and switch components to control lateral and polar flagellum rotation. J Bacteriol 184:2429–2438. https://doi.org/10.1128/jb.184.9.2429-2438.2002.
75. Paulick A, Delalez NJ, Brenzinger S, Steel BC, Berry RM, Armitage JP, Thormann KM. 2015. Dual stator dynamics in the *Shewanella oneidensis* MR-1 flagellar motor. Mol Microbiol 96:993–1001. https://doi.org/10.1111/mmi.12984.
76. Worning P, Jensen LJ, Nelson KE, Brunak S, Ussery DW. 2000. Structural analysis of DNA sequence: evidence for lateral gene transfer in *Thermotoga maritima*. Nucleic Acids Res 28:706–709. https://doi.org/10.1093/nar/28.3.706.
77. Eveleigh RJM, Meehan CJ, Archibald JM, Beiko RG. 2013. Being *Aquifex aeolicus*: untangling a hyperthermophile's checkered past. Genome Biol Evol 5:2478–2497. https://doi.org/10.1093/gbe/evt195.
78. Dibrova DV, Galperin MY, Koonin EV, Mulkidjanian AY. 2015. Ancient systems of sodium/potassium homeostasis as predecessors of membrane bioenergetics. Biochemistry (Mosc) 80:495–516. https://doi.org/10.1134/S0006297915050016.
79. Meier T, Krah A, Bond PJ, Pogoryelov D, Diederichs K, Faraldo-Gómez JD. 2009. Complete ion-coordination structure in the rotor ring of Na^+-dependent F-ATP synthases. J Mol Biol 391:498–507. https://doi.org/10.1016/j.jmb.2009.05.082.
80. Mulkidjanian AY, Galperin MY, Makarova KS, Wolf YI, Koonin EV. 2008. Evolutionary primacy of sodium bioenergetics. Biol Direct 3:13. https://doi.org/10.1186/1745-6150-3-13.
81. Gadsby DC. 2009. Ion channels versus ion pumps: the principal difference, in principle. Nat Rev Mol Cell Biol 10:344–352. https://doi.org/10.1038/nrm2668.
82. Gabel CV, Berg HC. 2003. The speed of the flagellar rotary motor of *Escherichia coli* varies linearly with protonmotive force. Proc Natl Acad Sci U S A 100:8748–8751. https://doi.org/10.1073/pnas.1533395100.
83. Gennis RB. 1989. Biomembranes: molecular structure and function. Springer-Verlag. New York, NY.
84. Armstrong CM, Hollingworth S. 2018. A perspective on Na and K channel inactivation. J Gen Physiol 150:7–18. https://doi.org/10.1085/jgp.201711835.
85. Kojima S, Takao M, Almira G, Kawahara I, Sakuma M, Homma M, Kojima C, Imada K. 2018. The helix rearrangement in the periplasmic domain of the flagellar stator B subunit activates peptidoglycan binding and ion influx. Structure 26:590–598.e5. https://doi.org/10.1016/j.str.2018.02.016.
86. Mandadapu KK, Nirody JA, Berry RM, Oster G. 2015. Mechanics of

torque generation in the bacterial flagellar motor. Proc Natl Acad Sci U S A 112:E4381–E4389. https://doi.org/10.1073/pnas.1501734112.
87. Morimoto YV, Minamino T. 2014. Structure and function of the bi-directional bacterial flagellar motor. Biomolecules 4:217–234. https://doi.org/10.3390/biom4010217.
88. Berg HC. 2000. Constraints on models for the flagellar rotary motor. Philos Trans R Soc Lond B Biol Sci 355:491–501. https://doi.org/10.1098/rstb.2000.0590.
89. Meister M, Lowe G, Berg HC. 1987. The proton flux through the bacterial flagellar motor. Cell 49:643–650. https://doi.org/10.1016/0092-8674(87)90540-x.
90. Onoue Y, Iwaki M, Shinobu A, Nishihara Y, Iwatsuki H, Terashima H, Kitao A, Kandori H, Homma M. 2019. Essential ion binding residues for Na^+ flow in stator complex of the *Vibrio* flagellar motor. Sci Rep 9:11216. https://doi.org/10.1038/s41598-019-46038-6.
91. Doyle DA. 2004. Structural changes during ion channel gating. Trends Neurosci 27:298–302. https://doi.org/10.1016/j.tins.2004.04.004.
92. Fillingame RH, Steed PR. 2014. Half channels mediating H^+ transport and the mechanism of gating in the F_o sector of *Escherichia coli* F_1F_o ATP synthase. Biochim Biophys Acta 1837:1063–1068. https://doi.org/10.1016/j.bbabio.2014.03.005.
93. Guo H, Suzuki T, Rubinstein JL. 2019. Structure of a bacterial ATP synthase. Elife 8:e43128. https://doi.org/10.7554/eLife.43128.
94. Celia H, Noinaj N, Zakharov SD, Bordignon E, Botos I, Santamaria M, Barnard TJ, Cramer WA, Lloubes R, Buchanan SK. 2016. Structural insight into the role of the Ton complex in energy transduction. Nature 538:60–65. https://doi.org/10.1038/nature19757.
95. Maki-Yonekura S, Matsuoka R, Yamashita Y, Shimizu H, Tanaka M, Iwabuki F, Yonekura K. 2018. Hexameric and pentameric complexes of the ExbBD energizer in the Ton system. Elife 7:e35419. https://doi.org/10.7554/eLife.35419.
96. Zhang X-Z, Goemaere EL, Seddiki N, Célia H, Gavioli M, Cascales E, Lloubes R. 2011. Mapping the interactions between *Escherichia coli* TolQ transmembrane segments. J Biol Chem 286:11756–11764. https://doi.org/10.1074/jbc.M110.192773.
97. Agrebi R, Wartel M, Brochier-Armanet C, Mignot T. 2015. An evolutionary link between capsular biogenesis and surface motility in bacteria. Nat Rev Microbiol 13:318–326. https://doi.org/10.1038/nrmicro3431.
98. Luoto HH, Belogurov GA, Baykov AA, Lahti R, Malinen AM. 2011. Na^+-translocating membrane pyrophosphatases are widespread in the microbial world and evolutionarily precede H^+-translocating pyrophosphatases. J Biol Chem 286:21633–21642. https://doi.org/10.1074/jbc.M111.244483.
99. Paula S, Volkov AG, Van Hoek AN, Haines TH, Deamer DW. 1996. Permeation of protons, potassium ions, and small polar molecules through phospholipid bilayers as a function of membrane thickness. Biophys J 70:339–348. https://doi.org/10.1016/S0006-3495(96)79575-9.
100. Beeby M, Ribardo DA, Brennan CA, Ruby EG, Jensen GJ, Hendrixson DR. 2016. Diverse high-torque bacterial flagellar motors assemble wider stator rings using a conserved protein scaffold. Proc Natl Acad Sci U S A 113:E1917–E1926. https://doi.org/10.1073/pnas.1518952113.
101. Chaban B, Coleman I, Beeby M. 2018. Evolution of higher torque in *Campylobacter*-type bacterial flagellar motors. Sci Rep 8:97. https://doi.org/10.1038/s41598-017-18115-1.
102. Chen S, Beeby M, Murphy GE, Leadbetter JR, Hendrixson DR, Briegel A, Li Z, Shi J, Tocheva EI, Müller A, Dobro MJ, Jensen GJ. 2011. Structural diversity of bacterial flagellar motors. EMBO J 30:2972–2981. https://doi.org/10.1038/emboj.2011.186.
103. Liu J, Lin T, Botkin DJ, McCrum E, Winkler H, Norris SJ. 2009. Intact flagellar motor of *Borrelia burgdorferi* revealed by cryo-electron tomography: evidence for stator ring curvature and rotor/C-ring assembly flexion. J Bacteriol 191:5026–5036. https://doi.org/10.1128/JB.00340-09.
104. Chang Y, Moon KH, Zhao X, Norris SJ, Motaleb MA, Liu J. 2019. Structural insights into flagellar stator-rotor interactions. Elife 8:e48979. https://doi.org/10.7554/eLife.48979.
105. Kojima S, Imada K, Sakuma M, Sudo Y, Kojima C, Minamino T, Homma M, Namba K. 2009. Stator assembly and activation mechanism of the flagellar motor by the periplasmic region of MotB. Mol Microbiol 73:710–718. https://doi.org/10.1111/j.1365-2958.2009.06802.x.
106. Søgaard-Andersen L. 2011. Directional intracellular trafficking in bacteria. Proc Natl Acad Sci U S A 108:7283–7284. https://doi.org/10.1073/pnas.1104616108.